Available online at www.sciencedirect.com
ScienceDirect
Infrared Physics & Technology 51 (2008) 160–167
INFRARED PHYSICS & TECHNOLOGY
www.elsevier.com/locate/infrared

Definition of a new thermal contrast and pulse correction for defect quantification in pulsed thermography

Hernán D. Benítez [a,*], Clemente Ibarra-Castanedo [b], AbdelHakim Bendada [b], Xavier Maldague [b], Humberto Loaiza [a], Eduardo Caicedo [a]

[a] Universidad del Valle, School of Electrical Engineering, Calle 13 Cra 100 Cali, Colombia
[b] Université Laval, Computer Vision and Systems Laboratory, Québec City, Québec, Canada G1K7P4

Received 30 October 2006
Available online 24 March 2007

Abstract

It is well known that the methods of thermographic non-destructive testing based on the thermal contrast are strongly affected by non-uniform heating at the surface. Hence, the results obtained from these methods considerably depend on the chosen reference point. The differential absolute contrast (DAC) method was developed to eliminate the need of determining a reference point that defined the thermal contrast with respect to an *ideal* sound area. Although, very useful at early times, the DAC accuracy decreases when the heat front approaches the sample rear face. We propose a new DAC version by explicitly introducing the sample thickness using the thermal quadrupoles theory and showing that the new DAC range of validity increases for long times while preserving the validity for short times. This new contrast is used for defect quantification in composite, Plexiglas™ and aluminum samples.

PACS: 81.70.Fy

Keywords: Thermographic non-destructive testing; Reference-free thermal contrast; Thermal quadrupoles

1. Introduction

Thermal contrast is used in non-destructive testing (NDT) by infrared thermography to evaluate defect visibility, enhance image quality and ultimately for quantitative purposes. Several types of contrasts have been defined such as absolute contrast, running contrast, normalized contrast and standard contrast [1–3]. All these contrast definitions require the use of the temperature in a sound area whose definition is a critical issue. In a wide sense, its location is not precisely identified since it may not be known in advance where the defects are, if present at all. Only assumptions can be made about the sound areas. This is the main limitation that can complicate the application of thermal contrast methods. However, in specific applications and materials the thermal contrast approach could be enough for obtaining proper quantitative results, without making just assumptions [4].

Moreover, it is well known that defect quantification methods based on thermal contrast are strongly affected by non-uniform heating [5]. The differentiated absolute contrast (DAC) method was developed to perform a more convenient computation of the sound area temperature based on the 1D solution of the Fourier equation for homogeneous and semi-infinite materials stimulated with a heat Dirac pulse [6,7]. This solution is given by Eq. (1):

$$\Delta T(t)_{\text{semi-infinite-body}}(x=0,t)=\frac{Q}{b\sqrt{\pi t}} \tag{1}$$

where Q is the energy density (J/m^2), b is thermal effusivity and t is time. Taking the thermogram obtained at time

* Corresponding author. Tel.: +57 2 339 17 80x112–116; fax: +57 2 339 21 40.
E-mail address: hbenitez@univalle.edu.co (H.D. Benítez).

1350-4495/$ - see front matter © 2007 Elsevier B.V. All rights reserved.
doi:10.1016/j.infrared.2007.01.001

t', which is a given value of time t ranging between the time of flash pulse and the time at which the first defect becomes visible, the temperature of the sound area $T(t')_s$ can be obtained from:

$$T(t')_s = \frac{Q}{b\sqrt{\pi t'}} \tag{2}$$

Combining equations Eqs. (1) and (2) the sound area temperature and DAC can be calculated as follows:

$$T_s = \sqrt{\frac{t'}{t}}T(t') \tag{3}$$

$$\Delta T_{DAC} = T(t) - \sqrt{\frac{t'}{t}}T(t') \tag{4}$$

This model does not include the sample thickness therefore the DAC accuracy decreases for long times after heating when the heat front reaches the sample face opposite to irradiation. In addition, strictly speaking, this approach is only valid for the case of shallow defects and/or thick samples.

In this article we propose a modified DAC version by explicitly introducing the sample thickness by means of the thermal quadrupoles theory [8]. We demonstrate that taking into account the sample thickness, the DAC validity range can be extended for long times after excitation while preserving its performance for short times. In this work planar and non-planar carbon fiber reinforced plastic (CFRP) composites with inserts are quantitatively evaluated by the new contrast method. Moreover, the new method is tested on Plexiglas™ and aluminum samples with flat bottom holes to estimate defect depth.

2. DAC modification using thermal quadrupoles

The thermal quadrupoles method is a Laplace transform based technique to explicitly represent linear systems and it is used to solve heat transfer problems. This method transforms the differential equations from the time-space domain representation to a Laplace domain representation that exhibits a very simple explicit form. After applying the Laplace transform, the problem can be solved in Laplace domain a then be transformed into the original time-space domain by inverse Laplace transform [9]. This method is used for direct problem solution (to calculate the thermal response in a system) and inverse problem solution (to estimate system parameters based on thermal response) [2,10–13]. Making use of the previously mentioned characteristics we carried out a study of a limited thickness non-transparent plate excited with a heat Dirac pulse to find the temperature distribution on the heated face (front face).

Fig. 1 shows a plate with thickness L (m) whose front face ($x = 0$) is excited with a heat Dirac pulse with energy density Q (J/m^2) while its rear face ($x = L$) is thermically isolated. If we define $T(x,t)$ and $\varphi(z,t)$ as the temperature and heat flux density in this 1D transient problem and if $\Theta(x,p)$ and $\Phi(x,p)$ are their Laplace transforms, where p

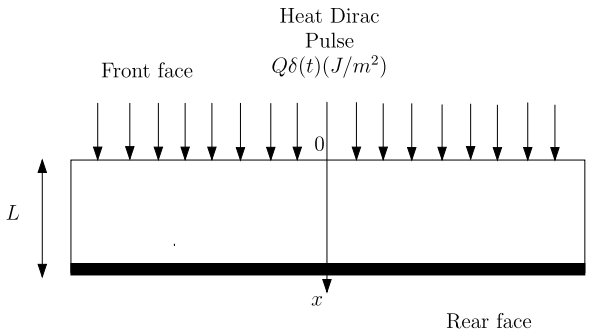

Fig. 1. Limited thickness plate excited with a heat Dirac pulse.

is the Laplace variable, it can be shown [14] that the slab of thickness L and zero uniform initial temperature behaves as a quadrupole:

$$\begin{pmatrix} \Theta_i \\ \Phi_i \end{pmatrix} = \mathbf{M}\begin{pmatrix} \Theta_o \\ \Phi_o \end{pmatrix} \quad \text{i: input, o: output} \tag{5}$$

with

$$\mathbf{M} = \begin{pmatrix} A & B \\ C & D \end{pmatrix} \tag{6}$$

and

$$\begin{aligned} A = D &= \cosh(kL), \quad C = \lambda k \sinh(kL) \\ B &= \sinh(kL)/(\lambda k), \quad k = \sqrt{p/\alpha} \end{aligned} \tag{7}$$

where λ is the thermal conductivity. The system in Eq. (5) can be expressed as:

$$\Theta_i = A\Theta_o + B\Phi_o \tag{8}$$

$$\Phi_i = C\Theta_o + D\Phi_o \tag{9}$$

Taking into account that $\Phi_i = Q$ and $\Phi_o = 0$ because of the isolation in the rear face, the Eq. (8) can be solved for Θ_i (front face temperature) as follows:

$$\Theta_i = \frac{QA}{C} = \frac{Q}{b}\frac{\coth\sqrt{\frac{pL^2}{\alpha}}}{\sqrt{p}} \tag{10}$$

Now the modified DAC deduction will be explained. The temperature in the time domain at times t and t' can be found by using the inverse Laplace transform:

$$T(t) = \frac{Q}{b}L^{-1}\left[\frac{\coth\sqrt{\frac{pL^2}{\alpha}}}{\sqrt{p}}\right]\Bigg|_t \tag{11}$$

$$T(t') = \frac{Q}{b}L^{-1}\left[\frac{\coth\sqrt{\frac{pL^2}{\alpha}}}{\sqrt{p}}\right]\Bigg|_{t'} \tag{12}$$

From Eq. (12) we can derive that

$$\frac{Q}{b} = \frac{T(t')}{L^{-1}\left[\frac{\coth\sqrt{\frac{pL^2}{\alpha}}}{\sqrt{p}}\right]\Big|_{t'}} \tag{13}$$

Replacing Eq. (13) in Eq. (11) we get:

$$\frac{T(t)}{T(t')} = \frac{L^{-1}\left[\frac{\coth\sqrt{\frac{pL^2}{\alpha}}}{\sqrt{p}}\right]\Big|_t}{L^{-1}\left[\frac{\coth\sqrt{\frac{pL^2}{\alpha}}}{\sqrt{p}}\right]\Big|_{t'}} \tag{14}$$

$$\Delta T_{\mathrm{DACcorr}} = T(t) - \frac{L^{-1}\left[\frac{\coth\sqrt{\frac{pL^2}{\alpha}}}{\sqrt{p}}\right]\Big|_t}{L^{-1}\left[\frac{\coth\sqrt{\frac{pL^2}{\alpha}}}{\sqrt{p}}\right]\Big|_{t'}} T(t') \tag{15}$$

The corrected DAC in Eq. (15) explicitly contains the specimen thickness L and does not depend on the heat density Q [15]. In this section we explained the methodology to deduce the corrected DAC, in the next section the experimental validation of corrected DAC will be shown.

3. Experimental validation

3.1. Experimental setup and specimens

Four experiments were carried out on four different samples to validate the proposed method. These experiments were performed using two photographic flashes (Balcar FX 60, 6.4 kJ), with a 5 ms pulse as the excitation source. All the thermogram sequences were recorded using a FPA infrared camera (Santa Barbara Focalplane SBF125, 3–5 μm), with a 320×256 pixel array. Two of the specimens are made of CFRP with planar and curved shapes as shown in Figs. 2 and 3. In each CFRP specimen, twenty-five (25) square Teflon™ insertions of different sizes were placed between plies at different locations as indicated. Each CFRP specimen is 2 mm thick. The other two specimens are made of Plexiglas™ and aluminum with circular flat bottom holes at different depths as indicated in Figs. 4 and 5. The Plexiglas specimen is 4 mm thick.

3.2. Quantification results

The main parameters used for sample inspection are described in Table 1. Thermal diffusivities (α) for each material were experimentally obtained by using the single side flash method described in [19] in which the solution of the front side is multiplied by the cube root of the time t. This function presents a minimum at $F_o = 0.2656$

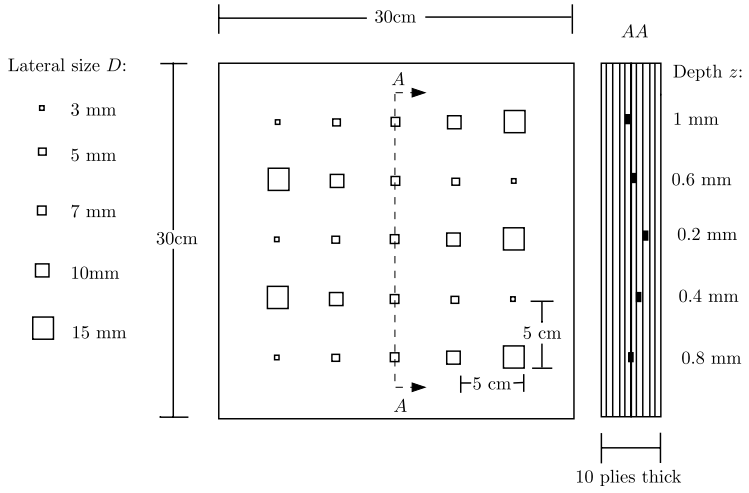

Fig. 2. Planar CFRP sample (CFRP006) with Teflon™ insertions.

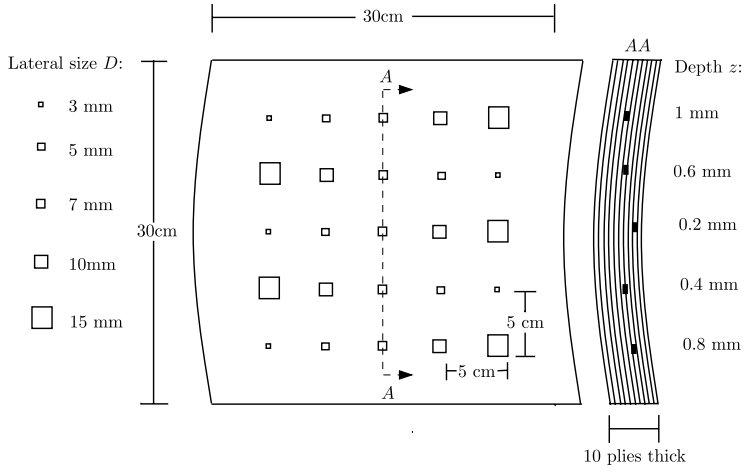

Fig. 3. Curved CFRP sample (CFRP007) with Teflon™ insertions.

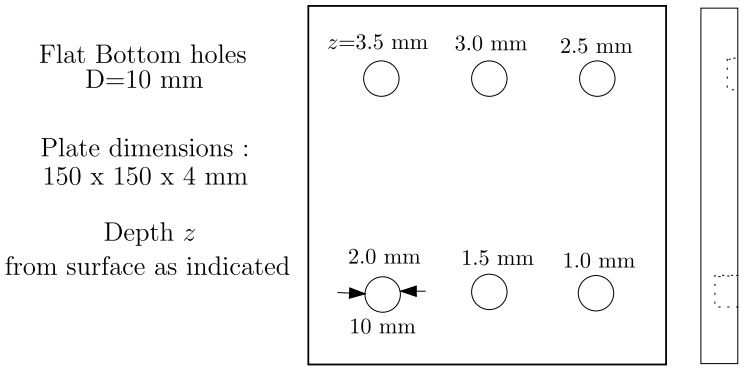

Fig. 4. Plexiglas™ sample (PLEXI014) with flat bottom holes.

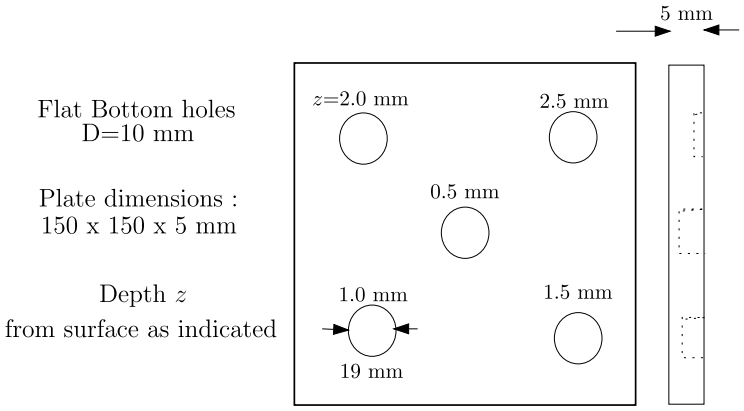

Fig. 5. Aluminum sample (ALUM02) with flat bottom holes.

Table 1
Parameters used for samples inspection

Specimen	$\alpha(\frac{m^2}{s} \times 10^{-7})$	t_s (ms)	Time vector (s)	t' (ms)
CFRP006	4.6	6.3	1e–4:6.3e–3:6.24	31.6
CFRP007	3.9	6.3	1e–4:6.3e–3:6.27	19
PLEXI014	0.6	880	1e–4:0.880:533.3	3600
ALUM02	430	6.3	1e–4:6.3e–3:6.06	0.1

$(F_o = \frac{\alpha t}{L^2})$ giving the following relation for the diffusivity measurement:

$$\alpha = \frac{0.2656\, L^2}{t_{min}} \tag{16}$$

where t_{min} is the time at which the global minimum is reached. t_s is the sampling time used for acquisition which is the same for CFRP and aluminum samples. However, for the Plexiglas™ sample the t_s is higher (880 ms) given its low thermal diffusivity (0.6e–7 $\frac{m^2}{s}$). The time vector is the set of time values used for the evaluation of Eq. (15).

Figs. 6 and 7 present the corrected DAC curves for insertions with diameter $D = 15$ mm in samples CFRP006 and CFRP007. Fig. 8 shows the curves extracted for insertions with diameter $D = 15$ mm in sample CFRP006 in which the classical DAC was applied. It is important to

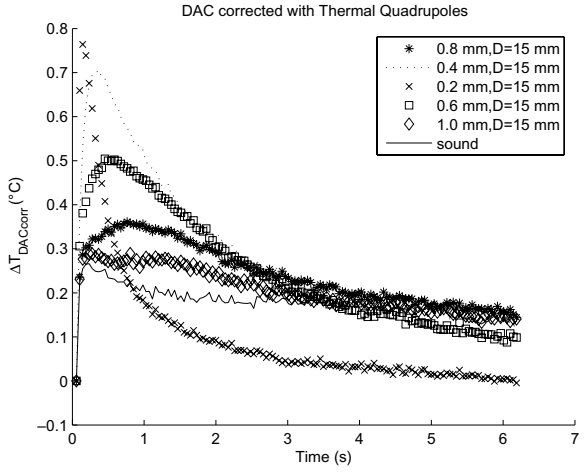

Fig. 6. Modified DAC curves for the five largest defects at different depths (15 mm in lateral size) in CFRP006.

observe that for times at the image sequence end (approximately $t \geqslant 2.5$ s) the validity of this DAC is not preserved since the contrast values increase instead of decreasing.

Defect depths from these composite samples were extracted from the following expression [16]:

$$z_{def} = 0.6722(\sqrt{t_{max}})(C_{max})^{-0.258} \tag{17}$$

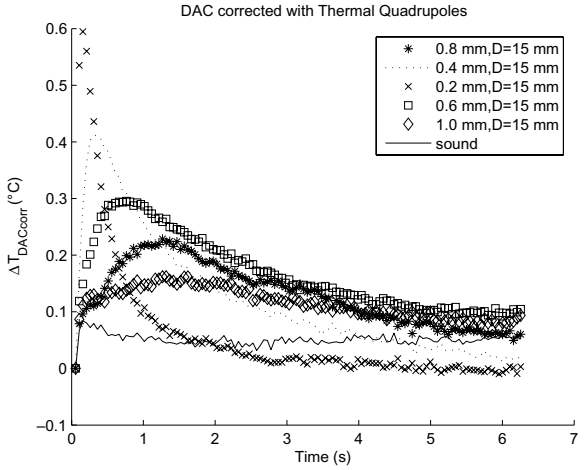

Fig. 7. Modified DAC curves for the five largest defects at different depths (15 mm in lateral size) in CFRP007.

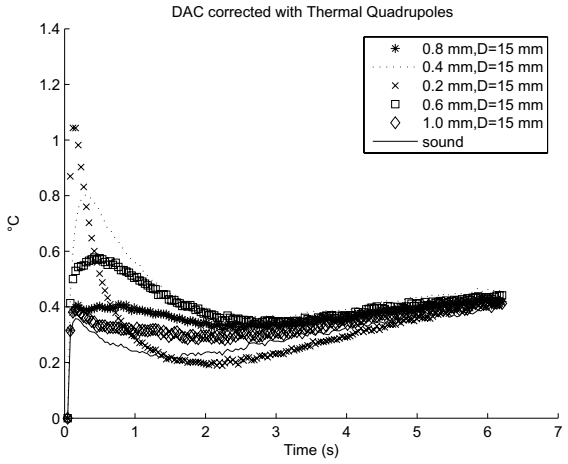

Fig. 8. Classic DAC curves for CFRP006.

where z_{def} is defect depth, t_{max} is the time at which the maximum thermal contrast C_{max} is reached.

Tables 2 and 3 summarize the quantification results and the % error for every defect in these samples. The % error is calculated as follows for all the inspected samples:

$$\%\text{error} = \frac{z_{est} - z}{z} \tag{18}$$

As can be observed, the defect size to depth ratio affects thermal contrast parameters t_{max}, C_{max} and defect depth estimation. It is important to mention that defect size to depth ratio was relatively large in the cases of composites inspection ($\frac{D}{z} \geqslant 3$). For instance, for insertions of size 3 mm and depths 0.8 mm and 1 mm the % error reaches values of 50% and 60% in CFRP006 and 32% and 50% in CFRP007. In addition, the anisotropy of the material and the uncertainty on the thermal properties might contribute to errors as well. Besides these uncertainities the estimation of z is affected by the correct correspondence between the time values during the experiment and the time

Table 2
Estimated depths and % error for all defects in sample CFRP006 using the corrected DAC

z (mm)	D (mm)	C_{max} (°C)	t_{max} (s)	z_{est} (mm)	Error (%)
0.2	15	0.36	0.77	0.25	20
0.4	15	0.71	0.25	0.37	−8
0.6	15	0.75	0.12	0.61	2
0.8	15	0.49	0.58	0.77	−4
1.0	15	0.28	0.85	0.86	−10
0.2	10	0.43	0.8	0.24	20
0.4	10	0.87	0.25	0.35	−10
0.6	10	1.00	0.13	0.6	−0.8
0.8	10	0.64	0.62	0.75	−6
1.0	10	0.33	0.8	0.8	−20
0.2	7	0.40	0.74	0.23	20
0.4	7	0.95	0.25	0.34	−20
0.6	7	1.2	0.13	0.56	−6
0.8	7	0.61	0.54	0.73	−9
1.0	7	0.36	0.75	0.76	−20
0.2	5	0.37	0.2	0.25	30
0.4	5	0.77	0.23	0.34	−10
0.6	5	0.89	0.13	0.37	−40
0.8	5	0.39	0.19	0.38	−50
1.0	5	0.31	0.78	0.8	−20
0.2	3	0.33	0.19	0.3	50
0.4	3	0.50	0.2	0.35	−10
0.6	3	0.49	0.14	0.41	−30
0.8	3	0.50	0.26	0.39	50
1.0	3	0.33	0.16	0.36	−60

Table 3
Estimated depths and % error for all defects in sample CFRP007 using the corrected DAC

z (mm)	D (mm)	C_{max} (°C)	t_{max} (s)	z_{est} (mm)	Error (%)
0.2	15	0.22	1.1	0.27	34
0.4	15	0.41	0.28	0.44	11
0.6	15	0.58	0.12	0.76	27
0.8	15	0.29	0.68	1.0	31
1.0	15	0.15	1.4	1.3	28
0.2	10	0.25	0.89	0.25	27
0.4	10	0.60	0.29	0.41	3.3
0.6	10	0.64	0.11	0.66	11
0.8	10	0.41	0.62	0.91	13
1.0	10	0.19	1.5	1.3	25
0.2	7	0.23	0.82	0.27	36
0.4	7	0.65	0.27	0.39	−2.5
0.6	7	0.60	0.13	0.66	10
0.8	7	0.39	0.6	0.89	11
1.0	7	0.19	0.93	1.0	0.23
0.2	5	0.19	0.78	0.28	39
0.4	5	0.45	0.25	0.41	2.2
0.6	5	0.50	0.12	0.71	18
0.8	5	0.27	0.57	0.91	14
1.0	5	0.16	0.79	0.96	−3.9
0.2	3	0.11	0.21	0.33	66
0.4	3	0.24	0.22	0.46	14
0.6	3	0.25	0.12	0.85	41
0.8	3	0.17	0.64	0.54	−32
1.0	3	0.12	0.17	0.48	−52

values (time vector) used for calculation of Eq. (15). This situation arises from the fact that correct t' determination is not always possible since the temperature values at the beginning of the acquisition is not reliable given the saturation of the camera.

Fig. 9 shows the corrected DAC curves for defects presented in PLEXI014 sample. These curves reach negative values at approximately 100 s due to convection losses.

The estimated defect depths z for PLEXI014 were calculated from expression:

$$z_{\text{def}} = 0.3416(\sqrt{t_{\max}})(C_{\max})^{-0.182} \tag{19}$$

This expression was deduced by finding the values $t_{\max}$ and $C_{\max}$ of corrected DAC curves described in Fig. 9 and fitting the data based on the formulas [1]:

$$z_{\text{def}} = A\sqrt{t_{\max}}(C_{\max})^{n} \tag{20}$$

$$\log\left[\frac{z_{\text{def}}}{\sqrt{t_{\max}}}\right] = \log(A) + n\log(C_{\max}) \tag{21}$$

Eq. (21) corresponds to the equation of a line from which values A and n can be easily extracted.

Table 4 describes the quantitative results for PLEXI014 specimen. The percentage of error obtained in this case is within the expected range of values being 8% the highest one. Moreover, this approach enables automated data analysis since no intervention with respect to the sound area choice is needed.

Fig. 10 shows the DAC curves for defects presented in ALUM02 sample. These curves reach the maximum value at the first instant of time. The estimated defects depths z_e showed in Table 5 were calculated from expression:

$$z_{\text{def}} = 38.61(\sqrt{t_{\max}})(C_{\max})^{-0.6} \tag{22}$$

This expression is deduced by following the same procedure to get Eq. (19). On the other hand, taking into account that the corrected DAC is based on the supposition that the heat stimulus is a Dirac pulse and that this stimulus in practice is long and have a complex shape, we propose a second modification to DAC introducing a correction in the heat stimulus shape. This second modification is important for DAC validity at short times when the inspected sample is a good heat conductor such as aluminum. The corrected temperature on the front face in Laplace domain is given by

$$\Theta(p)_{\text{corr}} = \Phi(p)\Theta(p) \tag{23}$$

The studied heat stimulus type is exponential (Fig. 11) described in time domain by [17]

$$\Phi(t) = \frac{t}{(t_f)^2}\mathrm{e}^{\frac{-t}{t_f}} \tag{24}$$

The Laplace transform of Eq. (24) is [18]:

$$\Phi(p) = \frac{1}{(p+\frac{1}{t_f})^2}\frac{1}{t_f^2} \tag{25}$$

where t_f is the impulsion baricenter.

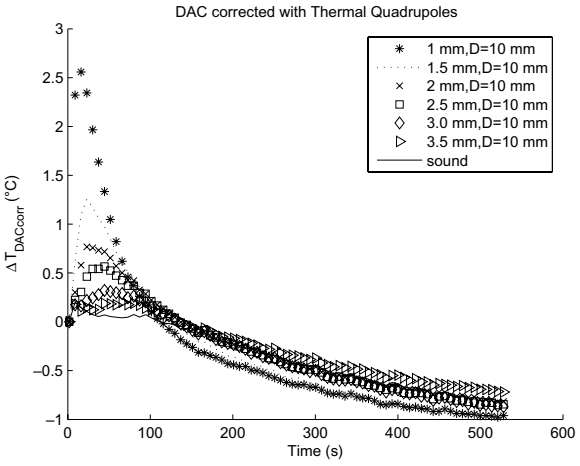

Fig. 9. Modified DAC curves for defects in Plexi014.

Table 4
Estimated depths and % error for all defects in sample PLEXI014 using the corrected DAC

z (mm)	D (mm)	$C_{\max}$ (°C)	$t_{\max}$ (s)	z_{est} (mm)	Error (%)
1	10	2.6	13	1.0	0
1.5	10	1.2	22	1.6	7
2.0	10	0.78	30	1.9	−5
2.5	10	0.55	37	2.3	−8
3.0	10	0.31	52	3.0	0
3.5	10	0.2	63	3.6	3

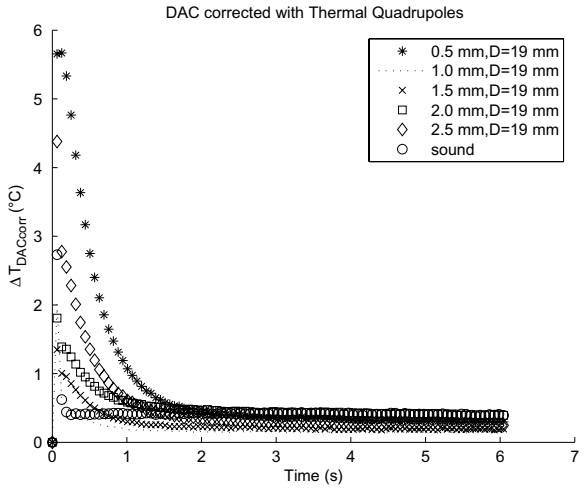

Fig. 10. Modified DAC curves for defects in ALUM02.

Table 5
Estimated depths and % error for all defects in sample ALUM02 using the corrected DAC

z (mm)	D (mm)	$C_{\max}$ (°C)	$t_{\max}$ (s)	z_{est} (mm)	Error (%)
0.5	19	7.8	0.0001	1.3	160
1.0	19	7.6	0.0001	1.3	27
1.5	19	4.8	0.0001	0.96	−36
2.0	19	8.3	0.0001	1.3	−33
2.5	19	13.0	0.0001	1.8	−29

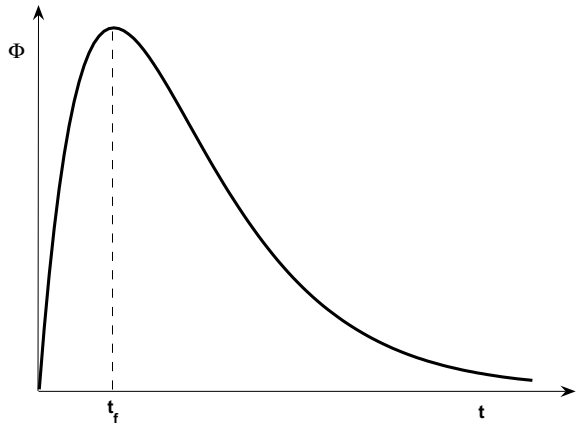

Fig. 11. Exponential heat pulse.

Replacing Eq. (25) in Eq. (23) gives

$$\Theta(p)_{\text{corr}} = \frac{1}{(p+\frac{1}{t_f})^2}\frac{1}{t_f^2}\frac{Q}{b}\frac{\coth\sqrt{\frac{pL^2}{\alpha}}}{\sqrt{p}} \tag{26}$$

Eq. (26) explicitly contains the baricenter of heat stimulus.

The values tested for t_s ranged from 2.5e–3 s to 1e–5 s showing that correct depth estimation results were obtained as long as t_s gets shorter proving that the heat pulse duration in the experiment approximated well the behavior of a Dirac pulse. The quantitative results obtained with $t_s = 1e{-}5$ show that the highest absolute error 160%! is presented for the shallowest defect (0.5 mm) while the depth estimation for the other defects reaches absolute errors of 35%. In this case depth estimation accuracy could be corrected with a higher sampling rate since the $t_{\max}$ for all the DAC curves were equal.

4. Conclusions

The modified DAC was tested with different materials in order to carry out depth estimation of defect type circular flat bottom holes in Plexiglas™ and aluminum and ribbon like delaminations in CFRP. The depth inversion procedure was performed by using the relation of defect depth z with the maximum contrast $C_{\max}$ and the time at which this maximum contrast is reached $t_{\max}$. The thermal contrast was obtained by pulsed thermography hence fast and relatively simple acquisition is achieved. However, special attention must be provided to the influence of the initial time of acquisition which is a source of incertitude to the measurement because of camera saturation. Experimental data showed that surface geometry have little impact on depth inversion results as shown with the test of CRPF007 which has a curved surface. The proposed corrected DAC approach can be considered an interesting alternative to thermal contrast computations since it provides an automated tool for depth retrieval and eliminates the need of selecting a non-defective area. Also this DAC technique reduces the impact of non-uniform heating, emissivity variations, environmental reflections and surface complex or non-planar geometry and eliminates as well the variability in thermal contrast calculations caused by these problems (since a local no defective area is used). Finally, this approach can be used in other methods such as the detection and quantification of defects with Artificial Neural Networks in which the modified DAC curves are used as training and validation data [20] and Pulsed Phase Thermography in which is necessary the a priori selection of a non-defective area in order to calculate the blind frequency f_b, i.e. the frequency at which the phase contrast is high enough for a defect to be detected, and carry on depth estimation [21,22].

Acknowledgements

Special acknowledgment for financial support is extended to the Colombian Institute of Science and Technology COLCIENCIAS and Universidad del Valle.

References

[1] X. Maldague, Theory and Practice of Infrared Technology for Nondestructive Testing, Wiley Interscience, New York, USA, 2001.
[2] A. Bendada, D. Maillet, J.C. Batsale, A. Degiovanni, Reconstitution of a non-uniform interface thermal resistance by inverse heat conduction Application to infrared thermography testing, Inverse Probl. Eng. 6 (1998) 79–123.
[3] J.C Krapez, Thermal Contrasts in Pulsed Infrared Thermography, in: X. Maldague, P.O Moore (Eds.), Nondestructive Testing Handbook: Infrared and Thermal Testing, vol. 3, Colombus, USA, 2001.
[4] N.P. Avdelidis, D.P. Almond, Transient thermography as a through skin imaging technique for aircraft assembly: modelling and experimental results, J. Infrared Phys. Technol. 45 (2) (2004) 103–114.
[5] R.E. Martin, A.L. Gyekenyesi, S.M. Shepard, Interpreting the results of pulsed thermography data, Mater. Eval. 61 (5) (2003) 611–616.
[6] M. Pilla, M. Klein, X. Maldague, A. Salerno, New Absolute Contrast for Pulsed Thermography, in: D. Balageas, G. Busse, G.M. Carlomagno, S. Svaić (Eds.), Proceedings of the Quantitative Infrared Thermography, Dubrovnik, Croatia, 2002.
[7] D.A. González, C. Ibarra-Castanedo, M. Pilla, M. Klein, J.M. López-Higuera, X. Maldague, Automatic interpolated differentiated absolute contrast algorithm for the analysis of pulsed thermographic sequence, in: D. Balageas, G. Busse, G.M. Carlomagno, J.M. Buchlin (Eds.), Proceedings of the Seventh Conference on Quantitative Infrared Thermography, von Karman Institute, Rhode Saint Genése, Belgium, 2004, pp. H.16.1–H.16.6.
[8] D. Maillet, S. André, J.C. Batsale, A. Degiovanni, C. Moyne, Thermal Quadrupoles: Solving the Heat Equation Through Integral Transform, John Wiley and Sons, West Sussex, England, 2000.
[9] H. Stehfest, Remarks on algorithm 368: Numerical inversion of Laplace transforms, Commun. ACM 13 (1) (1970) 47–49.
[10] J.V. Beck, K.A. Woodbury, Inverse problems and parameter estimation: integration of measurements and analysis, Meas. Sci. Technol. 9 (1998) 839–847.
[11] D. Maillet, A.S. Houlbert, S. Didierjean, A.S. Lamine, A. Degiovanni, Non-destructive evaluation of delaminations in a laminate: part I identification by measurement of thermal contrast, Compos. Sci. Technol. 47 (1993) 137–153.
[12] V.P Vavilov, Advances in signal inversion with applications to infrared thermography, in: Proceedings of the NATO Advanced Research Workshop on Advances in Signal Processing for Nondestructive Evaluation of Materials, Québec City, Canada, 1994.

[13] C. Ibarra-Castanedo, D. González, F. Galmiche, X.P. Maldague, A. Bendada, Discrete signal transforms as a tool for processing and analyzing pulsed thermographic data, in: J. Miles, G.R. Peacock, K.M. Knettel (Eds.), Proceedings of the SPIE Thermosense XXVIII, vol. 6205, Orlando, USA, 2006.
[14] A. Degiovani, Conduction dans un tour multicouche avec sources: extension de la notion de quadripole, Int. J. Heat Mass Transfer 31 (1988) 553–557.
[15] H.D. Benítez, C. Ibarra-Castanedo, A. Bendada, X. Maldague, H. Loaiza, E. Caicedo, Modified differential absolute contrast using thermal quadrupoles for the nondestructive testing of finite thickness specimens by infrared thermography, in: Proceedings of the CCECE 2006 – Canadian conference on electrical and computer engineering, Ottawa, Canada, 2006.
[16] D.L. Balageas, A.A. Déom, D.M. Boscher, Characterization and nondestructive testing of carbon-epoxy composites by a pulsed photothermal method, Mater. Eval. 45 (4) (1987) 461–465.
[17] A. Degiovanni, Correction de longueur d'impulsion pour la mesure de la diffsivité thermique par méthode flash, Int. J. Heat Mass Transfer 30 (10) (1987) 2199–2200.
[18] S. Seely, Laplace transforms, in: A.D. Poularikas (Ed.), The Transforms and Applications Handbook, second ed., CRC Press LLC, Boca Raton, USA, 2000.
[19] F. Cernuschi, P.G. Bison, S. Marinetti, A. Figari, L. Lorenzoni, E. Grinzato, Comparison of thermal diffusivity measurement techniques, in: D. Balageas, G. Busse, G.M. Carlomagno, S. Vaic (Eds.), Proceedings of the Sixth Conference on Quantitative Infrared Thermography, Dubrovnik, Croatia, 2002.
[20] H.D. Benitez, C. Ibarra-Castanedo, H. Bendada, X. Maldague, H. Loaiza, E. Caicedo, Defect quantification with reference free thermal contrast and artificial neural networks, in: K.M. Knettel, V. Vavilov, J. Miles (Eds.), Proceedings of the SPIE Thermosense XXIX, vol. 6541, Orlando, USA, 2007.
[21] C. Ibarra-Castanedo, N.P. Avdelidis, E.G. Grinzato, P.G. Bison, S. Marinetti, L. Chen, M. Genest, X. Maldague, Quantitative inspection of non-planar composite specimens by pulsed phase thermography, Quant. Infrared Thermography J. 3 (1) (2006) 25–40.
[22] M. Susa, H.D. Benítez, C. Ibarra-Castanedo, H. Loaiza, H. Bendada, X. Maldague, Phase contrast using a differentiated absolute contrast method, Quant. Infrared Thermography J. 3 (2) (2006) 219–230.